Adsorption dynamics of bifunctional molecules: Allyl methyl ether on Si(001)

Tamam Bohamud, (iD) Ulrich Höfer and (iD) Michael Dürr

View Online   Export Citation   CrossMark

ARTICLES YOU MAY BE INTERESTED IN

Adsorption dynamics of bifunctional molecules: Allyl methyl ether on Si(001)

Tamam Bohamud,[1] Ulrich Höfer,[1] (iD) and Michael Dürr[1,2,a] (iD)

AFFILIATIONS

[1] Fachbereich Physik and Zentrum für Materialwissenschaften, Philipps-Universität Marburg, D-35032 Marburg, Germany

[2] Institut für Angewandte Physik and Zentrum für Materialforschung, Justus-Liebig-Universität Giessen, D-35392 Giessen, Germany

[a] Author to whom correspondence should be addressed: michael.duerr@ap.physik.uni-giessen.de

ABSTRACT

The reaction dynamics of allyl methyl ether (AME) on Si(001) was studied by means of molecular beam techniques. The reaction of this bifunctional molecule comprising an ether and an alkene group was found to proceed via an intermediate state as deduced from the temperature dependence of the initial sticking probability s_0. At constant surface temperature T_s, s_0 decreases continuously with increasing kinetic energy E_{kin}, indicating a non-activated adsorption channel. Qualitatively and quantitatively, the energy dependence is almost identical to the adsorption dynamics of diethyl ether on Si(001). We attribute this to a similar nature of the intermediate state, which largely determines the adsorption dynamics. In consequence, this indicates a predominant role of the ether group and a minor influence of the C=C double bond on the adsorption dynamics of AME on Si(001).

INTRODUCTION

Adsorption of organic molecules on the Si(001) surface typically proceeds via an intermediate state that is characterized by a relatively weak, non-covalent bond between the functional group of the adsorbing molecules and the surface. The type of the functional group thus determines the nature of the binding in the intermediate state,[1–4] which, in turn, governs the adsorption dynamics[5–9] (Fig. 1). The adsorption dynamics of alcohols and ethers on Si(001)[6,9] may serve as a good example: in both cases, the adsorbing molecules form a dative bond with the surface in the intermediate state[10–18] (lower right sketch in Fig. 1), and despite major differences in their structure, mass, and the energetics of the further reaction into the final state, they show almost identical adsorption dynamics as determined by the dependence of the initial sticking probability s_0 on the kinetic energy E_{kin} of the incoming molecules.[9] On the other hand, molecules with different functional groups such as alkenes feature a considerably stronger dependence of s_0 on E_{kin} and thus a much lower reactivity at high kinetic energy of the incident molecules[5] (Fig. 1). In the latter case, the intermediate state involves a weaker three-center bonding between the surface and the carbon–carbon

double bond of the alkene molecules[19–23] (upper right sketch in Fig. 1).

In the case of molecules with two or more functional groups, the reaction pathway was determined for a couple of systems,[3] both theoretically and experimentally. To the best of our knowledge, however, the effect of different functional groups on the adsorption dynamics of such bifunctional molecules has not been investigated so far.

In this paper, we study the adsorption dynamics of the bifunctional molecule allyl methyl ether (AME) on Si(001). Using molecular beam techniques for the adsorption experiments, the kinetic energy of the molecules impinging on the surface can be controlled, in contrast to adsorption from thermal gas. Whereas the latter experiments measure the kinetics of a reaction, e.g., at different surface temperatures, and give valuable information on the energetics of the reaction,[24–26] the molecular beam experiments exploit, in addition, the dynamics of the reaction in terms of the influence of the kinetic energy of the incoming molecules on the reactivity.[27]

The two functional groups in the AME molecule, i.e., the ether group with its oxygen heteroatom and the C=C double bond,
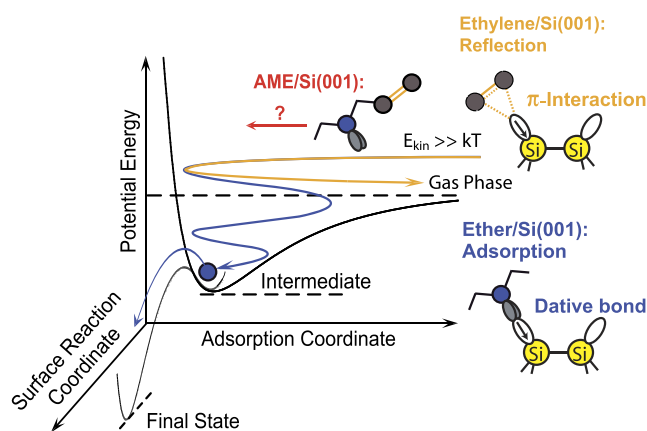
FIG. 1. Schematic representation of the potential energy surface of organic molecules on Si(001). Adsorption into the intermediate state and conversion from the intermediate into the final state are two largely decoupled processes as indicated by the two orthogonal reaction coordinates. The initial adsorption dynamics are thus determined by the intermediate state. As an example, molecules that adsorb in the intermediate state via a dative bond between, e.g., oxygen as a heteroatom and a Si surface atom (sketch in lower right), show a much higher probability for adsorption into the intermediate at increased kinetic energy when compared to, e.g., alkenes, which adsorb via a π complex involving the C=C double bond (sketch in upper right).

react via two very different intermediate states that exhibit different adsorption energetics and dynamics. We compare the results of AME to the adsorption dynamics of diethyl ether (Et_2O) and ethylene (C_2H_4) on Si(001) in order to disentangle the contribution of each functional group to the overall reaction dynamics. Despite the high reactivity of the C=C double bond on Si(001),[24,28–32] we show here that the adsorption dynamics is mainly determined by the ether group. The C=C double bond then influences the further reaction from the intermediate into the final state as deduced from the dependence of s_0 on surface temperature T_s.

METHODS

The experiment was described in detail in Refs. 27 and 33. In short, the experimental setup consists of a four stage molecular beam apparatus, and the beam is generated via supersonic expansion through a nozzle of 100 μm in diameter. The sample is located 30 cm downstream of the nozzle. The kinetic energy of the molecules in the beam was varied by heating the nozzle, seeding the beam in noble gas of different atomic mass (i.e., helium), or both seeding and heating of the nozzle. The mean kinetic energy and its distribution were determined by means of time-of-flight measurements. Typical values of the ratio between the mean velocity of the molecules and the width of the velocity distribution, i.e., the speed ratio S, range between $S = 2.5$ for the unseeded beam to $S = 11$ for the seeded beam of $E_{kin} = 550$ meV.

The sample was prepared by resistive heating up to 1300 K and subsequent cooling with cooling rates of ≈1 K/s. We verified the 2 × 1 reconstruction of the Si(001) surface by means of low energy electron diffraction. During the experiment, the sample was heated up to 1100 K between two successive adsorption measurements in order to desorb the adsorbates of the former measurement from the surface.

The temperature of the sample was measured using a thermocouple glued to the rear side of the sample.

The absolute sticking coefficient s was determined by means of the King-and-Wells method:[34] when the molecular beam enters the sample chamber and an inert shutter is placed in the front of the sample, the partial pressure related to the investigated molecules is increased due to the molecules being reflected from the inert shutter. The partial pressure is monitored by using a quadrupole mass spectrometer (QMS), which is positioned out of the line of sight of the molecular beam. The QMS was operated at $m/z = 45$, the most intense signal in the mass spectrum of AME. When the shutter is opened, a drop of the QMS signal is observed due to adsorption on the reactive sample surface. This drop of the partial pressure is proportional to the initial sticking coefficient $s_0 = s(t = 0)$ as long as the beam diameter (≈8 mm) is smaller than the sample surface, which is 5 × 1 cm^2 in size. From the raw data, the background partial pressure is subtracted. The latter is caused by thermal gas that enters the main chamber effusively via the aperture and can be measured by blocking the beam in the first differential pumping stage; it typically accounts for less than 5% of the total signal. After background subtraction, the absolute value of s_0 is determined from the initial signal drop when the data are normalized to the maximum value of the signal.

RESULTS

In Fig. 2, the adsorption measurements, which are represented by the partial pressure measured as a function of time, are shown for three different beam energies E_{kin} at a given surface temperature $T_s = 540$ K. The initial signal drop after opening the shutter at $t = 0$ s as indicated by the black arrows decreases with increasing E_{kin}. This implies a reduced initial sticking coefficient s_0 at higher E_{kin}. The kinetic energy was varied between 90 meV (unseeded
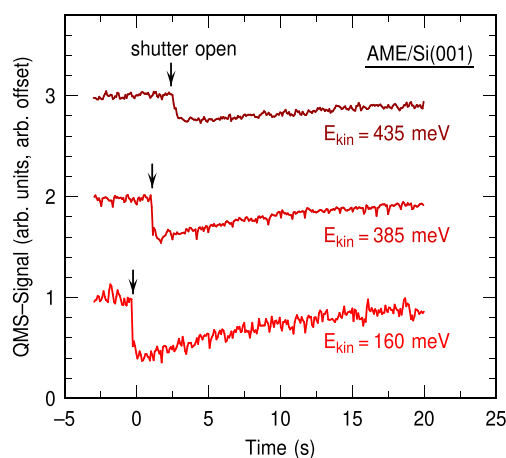
FIG. 2. Adsorption curves, i.e., normalized partial pressure as a function of time, measured for AME on Si(001) at a constant surface temperature $T_s = 540$ K and three different kinetic energies. When the inert shutter is opened (black arrows), the signal drops due to adsorption on the surface. In the further course of the experiment, the signal again increases as the surface coverage increases and the sticking probability s decreases.

beam) and 550 meV by seeding the beam and heating the nozzle to $T_N = 1000$ K.

The dependence of the initial sticking coefficient on kinetic energy is shown in Fig. 3 for two different surface temperatures. At low kinetic energy, the sticking coefficients exhibit the highest values, indicating a high sticking probability for the adsorption of thermal gas, in qualitative agreement with thermal gas adsorption measurements. With increasing E_{kin}, the initial sticking coefficient decreases continuously for a given surface temperature. For comparison, we additionally measured $s_0(E_{kin})$ for diethyl ether and further compare to the data for ethylene on Si(001) taken from Ref. 5. For Et_2O/Si(001) (blue lines, data shown in Fig. S1 in the supplementary material), the decrease in s_0 with increasing E_{kin} is very similar to AME/Si(001). For C_2H_4/Si(001) (ocher dashed-dotted line, from Ref. 5), s_0 drops much faster with increasing E_{kin} when compared to AME and Et_2O.

The dependence of the initial sticking coefficient on surface temperature was determined at a constant kinetic energy of E_{kin} = 90 meV (room temperature nozzle, unseeded beam). The results are shown in Fig. 4 (red data): s_0 is constant for $T_s < 400$ K and drops continuously at surface temperatures $T_s > 400$ K. This dependence indicates that the adsorption proceeds via an intermediate state: Once the impinging molecule is trapped in the intermediate state, it can either react into the final state or it desorbs back into the gas phase. For a non-activated reaction, the desorption barrier ϵ_d is higher than the conversion barrier ϵ_a; thus, at increased surface temperature, desorption is favored over conversion, leading to the drop of s_0. With ν_d and ν_a being the prefactors for the desorption and conversion rate, respectively, and $s_{0,max}$ being the probability for adsorption in the intermediate state, the temperature dependence of s_0 can be expressed according to the Kisliuk model[35] as
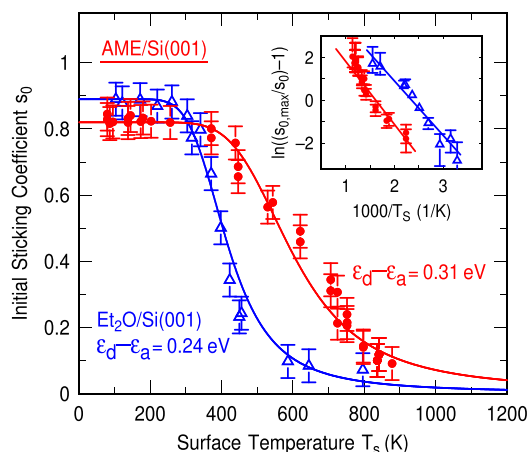

FIG. 3. Initial sticking coefficient as a function of the kinetic energy of the impinging molecules for AME (red data points and lines) and Et_2O (blue lines, data points in Fig. S1 in the supplementary material) on Si(001). Surface temperatures were chosen in order to obtain comparable absolute sticking probabilities s_0. In addition, the dependence of s_0 on E_{kin} for ethylene is shown (ocher dashed-dotted line, from Ref. 5).

FIG. 4. Initial sticking coefficient s_0 as a function of surface temperature for AME (red data points and line) and Et_2O on Si(001) (blue data points and line, taken from Ref. 36). (Inset) Kisliuk plot[35] for both datasets for fitting Eq. (1) to the data. The lines in the main graph represent the results obtained from fitting the Kisliuk model, as shown in the inset.

$$\ln\left(\frac{1}{s_0/s_{0,\,max}} - 1\right) = \ln\left(\frac{\nu_d}{\nu_a}\right) - \left(\frac{\epsilon_d - \epsilon_a}{k_B T_s}\right). \quad (1)$$

Fitting Eq. (1) to the data as shown in the inset of Fig. 4, the difference between the two energy barriers $\epsilon_d - \epsilon_a$ can be deduced. For AME/Si(001), we obtain $(\epsilon_d - \epsilon_a)_{AME}$ = 0.31 ± 0.04 eV. Despite the similarity of the dependence of s_0 on E_{kin} for AME and diethyl ether on Si(001), the $s_0(T_s)$ data of Et_2O/Si(001), which are shown in Fig. 4 as well (blue data, taken from Ref. 36), significantly deviate from the AME/Si(001) system. For Et_2O/Si(001), $(\epsilon_d - \epsilon_a)_{Et_2O}$ = 0.24 ± 0.04 eV was reported.[36]

DISCUSSION

We first discuss the continuous decrease in the initial sticking coefficient s_0 with increasing beam energy E_{kin}, as shown in Fig. 3. Such a dependence is typical for a non-activated adsorption channel. The higher the kinetic energy of the incoming molecules, the less likely it is that the molecules dissipate enough energy that they are trapped in the intermediate state. When comparing the results for AME and diethyl ether, it is obvious that both datasets follow the same functional form, i.e., a linear dependence of s_0 on E_{kin}. Moreover, the slopes are almost identical for comparable values of s_0. In contrast, the data for ethylene on Si(001) show a much stronger dependence of s_0 on E_{kin}. In a previous study, we have shown that the nature of the intermediate determines the adsorption dynamics.[8] As we observe almost identical adsorption dynamics for AME and diethyl ether, but very different adsorption dynamics in case of ethylene on Si(001), we conclude that in the case of the bifunctional molecule AME, the dynamics are largely determined by the ether group and the corresponding intermediate. The latter comprises a dative bond between the oxygen atom of the ether group
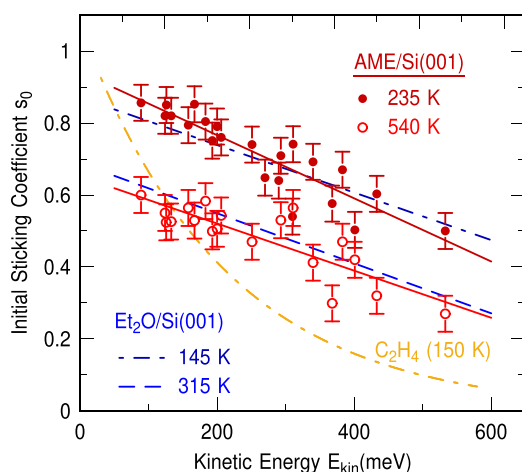
and the unfilled D_{down} state of a silicon dimer. This bond is relatively strong,[36] in particular, when compared to the three-center π complex, which is formed in the intermediate between the C=C double bond of ethylene and the unfilled D_{down} state of the silicon surface.[19,23] From our results, we conclude that the C=C double bond as a second functional group in the AME molecule does not significantly affect the adsorption dynamics into the intermediate state, which are governed by the ether group.

In our discussion, we made use of the fact that the nature of the intermediate determines the adsorption dynamics,[8,9] which enabled us to identify the reaction channel that governs the reaction of AME into the intermediate state. At this point, we would like to note that one can further exploit this observation to determine the reaction channels including the involved intermediate state also for molecules which do not give easy access to the intermediate state, e.g., in case it is too short-lived for the experimental techniques applied.

Although the C=C double bond in the AME molecule does not influence the adsorption dynamics into the intermediate, it has a non-negligible influence on the further reaction from the intermediate into the final state as deduced from the temperature dependence of the sticking probability: The energy difference $\epsilon_d - \epsilon_a = 0.31$ eV and the prefactor ratio $\frac{\nu_d}{\nu_a} = 3.8 \times 10^2$ for AME/Si(001) deviate significantly from the values measured for Et$_2$O/Si(001) ($\epsilon_d - \epsilon_a = 0.24$ eV, $\frac{\nu_d}{\nu_a} = 7 \times 10^{2\,[36]}$). This difference is attributed to the presence of the C=C double bond in the AME molecule, which is the major difference between the two molecules.

The further reaction of the ether group into the final state proceeds via the cleavage of the O—C bond ($\epsilon_a = 0.4$ eV in the case Et$_2$O[36]), leading to a Si—OCH$_2$CH$_3$ and a Si—CH$_2$CH$_3$ entity. The presence of the C=C functional group in the AME molecule may provide an additional reaction channel for the conversion from the intermediate into the final state via the [2 + 2] cycloaddition of C=C on silicon, which proceeds with a reduced barrier.[20] Indeed, the higher value of $\epsilon_d - \epsilon_a$ indicates a lower energy of the transition state between the intermediate and final state, which translates into a lower conversion barrier if we assume the same binding energy in the intermediate state for both molecules. Both the decreased transition state energy and the increased value for the ratio of the prefactors, $\frac{\nu_a}{\nu_d}$, are thus in line with an additional reaction channel for the further reaction into the final state, which might be a combination of the final states of the ether and the C=C entities.

CONCLUSION

The adsorption dynamics of the bifunctional molecule AME was found to be mainly determined by the ether group with a negligible influence of the C=C double bond. On the other hand, the further reaction into the final state deviates from the kinetics deduced for molecules with an ether functionality only, indicating a substantial influence of the C=C double bond in the further course of the reaction. The results thus demonstrate that the initial adsorption dynamics can be controlled by one functional group only even when the further reaction comprises both functional groups of a bifunctional molecule.

SUPPLEMENTARY MATERIAL

The supplementary material includes the data on the initial sticking probability for diethyl ether on Si(001) measured as a function of the kinetic energy of the incoming molecules.

DATA AVAILABILITY

The data that support the findings of this study are available from the corresponding author upon reasonable request.

REFERENCES

[1] M. A. Filler and S. F. Bent, Prog. Surf. Sci. **73**, 1 (2003).
[2] J. Yoshinobu, Prog. Surf. Sci. **77**, 37 (2004).
[3] T. R. Leftwich and A. V. Teplyakov, Surf. Sci. Rep. **63**, 1 (2008).
[4] J. H. G. Owen, J. Phys.: Condens. Matter **21**, 443001 (2009).
[5] M. A. Lipponer, N. Armbrust, M. Dürr, and U. Höfer, J. Chem. Phys. **136**, 144703 (2012).
[6] M. A. Lipponer, M. Dürr, and U. Höfer, Chem. Phys. Lett. **624**, 69 (2015).
[7] M. Reutzel, N. Münster, M. A. Lipponer, C. Länger, U. Höfer, U. Koert, and M. Dürr, J. Phys. Chem. C **120**, 26284 (2016).
[8] M. A. Lipponer, M. Reutzel, M. Dürr, and U. Höfer, Surf. Sci. **653**, 118 (2016).
[9] T. Bohamud, M. Reutzel, M. Dürr, and U. Höfer, J. Chem. Phys. **150**, 224703 (2019).
[10] T. Kato, S.-Y. Kang, X. Xu, and T. Yamabe, J. Phys. Chem. B **105**, 10340 (2001).
[11] R. Miotto, G. P. Srivastava, and A. C. Ferraz, RSC Adv. **575**, 287 (2005).
[12] Y. H. Min, H. Lee, D. H. Kim, and S. Kim, in *Functionalization of Semiconductor Surfaces*, 1st ed., edited by F. Tao and S. L. Bernasek (John Wiley & Sons, Hoboken, NJ, 2012), pp. 193–231.
[13] G. Mette, M. Reutzel, R. Bartholomäus, S. Laref, R. Tonner, M. Dürr, U. Koert, and U. Höfer, ChemPhysChem **15**, 3725 (2014).
[14] M. Reutzel, G. Mette, P. Stromberger, U. Koert, M. Dürr, and U. Höfer, J. Phys. Chem. C **119**, 6018 (2015).
[15] L. Pecher, S. Laref, M. Raupach, and R. Tonner, Angew. Chem., Int. Ed. **56**, 15150 (2017).
[16] C. Länger, T. Bohamud, J. Heep, T. Glaser, M. Reutzel, U. Höfer, and M. Dürr, J. Phys. Chem. C **122**, 14756 (2018).
[17] K. M. O'Donnell, C. Byron, G. Moore, L. Thomsen, O. Warschkow, A. Teplyakov, and S. R. Schofield, J. Phys. Chem. C **123**, 22239 (2019).
[18] G. Mette, A. Adamkiewicz, M. Reutzel, U. Koert, M. Dürr, and U. Höfer, Angew. Chem., Int. Ed. **58**, 3417 (2019).
[19] J.-H. Cho and L. Kleinman, Phys. Rev. B **69**, 075303 (2004).
[20] C.-H. Chung, W.-J. Jung, and I.-W. Lyo, Phys. Rev. Lett. **97**, 116102 (2006).
[21] K. T. Wong and S. F. Bent, in *Functionalization of Semiconductor Surfaces*, 1st ed., edited by F. Tao and S. L. Bernasek (John Wiley & Sons, Hoboken, NJ, 2012), pp. 51–88.
[22] K. Akagi and J. Yoshinobu, Surf. Sci. **652**, 304 (2016).
[23] J. Pecher, G. Mette, M. Dürr, and R. Tonner, ChemPhysChem **18**, 357 (2018).
[24] L. Clemen, R. M. Wallace, P. A. Taylor, M. J. Dresser, W. J. Choyke, W. H. Weinberg, and J. T. Yates, Surf. Sci. **268**, 205 (1992).
[25] Z. Ma and F. Zaera, Surf. Sci. Rep. **61**, 229 (2006).
[26] R. Coustel, Y. Borensztein, O. Pluchery, and N. Witkowski, Phys. Rev. Lett. **111**, 096103 (2013).
[27] M. Dürr and U. Höfer, Surf. Sci. Rep. **61**, 465 (2006).

[28] C. Huang, W. Widdra, and W. H. Weinberg, Surf. Sci. **315**, L953 (1984).

[29] J. Yoshinobu, H. Tsuda, M. Onchi, and M. Nishijima, J. Chem. Phys. **87**, 7332 (1987).

[30] F. Rochet, F. Jolly, F. Bournel, G. Dufour, F. Sirotti, and J.-L. Cantin, Phys. Rev. Lett. **58**, 11029 (1998).

[31] F. Matsui, H. W. Yeom, I. Matsuda, and T. Ohta, Phys. Rev. B **62**, 5036 (2000).

[32] G. Mette, C. H. Schwalb, M. Dürr, and U. Höfer, Chem. Phys. Lett. **483**, 209 (2009).

[33] M. Dürr and U. Höfer, Phys. Rev. Lett. **88**, 076107 (2002).

[34] D. A. King and M. G. Wells, Surf. Sci. **29**, 454 (1972).

[35] P. Kisliuk, J. Phys. Chem. Solids **3**, 95 (1957).

[36] M. Reutzel, M. Lipponer, M. Dürr, and U. Höfer, J. Phys. Chem. Lett. **6**, 3971 (2015).